Microbunching of relativistic electrons using a two-frequency laser

D. Gordon,[1] C. E. Clayton,[1] T. Katsouleas,[2] W. B. Mori,[1] and C. Joshi[1]
[1]*University of California at Los Angeles, Los Angeles, California 90095*
[2]*University of Southern California, Los Angeles, California 90089*
(Received 10 July 1997)

A high power two-frequency laser can be used to modulate the axial momentum of a copropagating relativistic electron beam. The net work done on each electron is accounted for almost entirely by the axial electric field of the laser even when approaching the one-dimensional limit. After interacting with the laser, the electron beam can be bunched either by a long drift space or a dispersive optic. We give an example in which a 2.5-TW CO_2 laser and a chicane compressor are used to transform a constant stream of 16-MeV electrons into a train of 60-fs microbunches, each containing 10 pC of charge. [S1063-651X(98)09601-9]

PACS number(s): 52.40.Nk, 52.20.Dq, 52.75.Di

I. INTRODUCTION

Many plasma based accelerators, such as the plasma beatwave accelerator [1], employ a periodic accelerating structure with a wavelength on the order of 100 μm. In order for such accelerators to produce monoenergetic beams, the injected particles must be confined to a small region of phase within each period of this structure. Femtosecond electron pulses are therefore needed. We propose a microbunching technique which generates such ultrashort electron pulses by exploiting the interaction between a two-frequency laser beam and a copropagating relativistic electron beam in vacuum. This interaction modulates the electron momentum at the frequency of the beat envelope associated with the interference of the two laser lines. The momentum-modulated electrons can subsequently be transformed into a train of microbunches using a magnetic compression scheme. This approach could be particularly advantageous when applied to the plasma beatwave accelerator because the same laser could both bunch the injected particles and drive the plasma wave accelerating structure. The electron bunches would then be automatically timed such that they are all injected at equivalent phases of the plasma wave.

The process described above falls into the general category of the acceleration of charged particles by intense laser fields in vacuum, which has been the subject of active research for many years. In fact, a problem similar to the one analyzed here has been discussed in the papers by Sprangle *et al.* [2] and Esaray *et al.* [3], and was further elaborated upon by Hafizi *et al.* [4]. In these papers it was proposed that relativistic electrons could be substantially accelerated by copropogating them with a high power two-frequency laser. The problem was analyzed both analytically and via three-dimensional numerical simulations.

The problem presented here is related to the one presented in Refs. [2–4] as follows. In both cases, the change in the energy of an electron propagating coaxially with a two-frequency laser is to be determined. This quantity is given in both cases by integrating an expression of the form

$$\frac{d\gamma}{dz}=\frac{F(z)}{\gamma}, \tag{1}$$

where γ is the relativistic Lorentz factor of the electron. In Refs. [2–4], $F(z)$ was determined by neglecting the excursion of the electron away from the axis during its quiver motion. This implied that the effects of the axial laser field, E_z, were not considered. The validity of this model was supported by numerical calculations which did take E_z into account. In this work, we consider a regime where E_z cannot be neglected. An analytical solution is found for the energy change due to E_z, and an analytical scaling is found for the importance of E_z relative to the $\mathbf{v}\times\mathbf{B}$ force.

The regime investigated in this paper differs further from the one investigated in Refs. [2–4] in that we consider a small perturbation to the electron energy, while Refs. [2–4] considered a drastic energy change. These are both special cases of a more general analysis. To see this, rewrite Eq. (1) as follows:

$$\frac{1}{2}\frac{d}{dz}\gamma^2=F(z). \tag{2}$$

Next, let $\gamma=\gamma_0+\delta\gamma$, where γ_0 is the relativistic Lorentz factor prior to the interaction (i.e., at $z=-\infty$). Then,

$$\gamma_0\frac{d}{dz}\delta\gamma+\frac{1}{2}\frac{d}{dz}\delta\gamma^2=F(z). \tag{3}$$

If $\delta\gamma$ is sufficiently large, the first term can be neglected, and the energy change will scale as $P^{1/2}$, where P is the laser power. This was the case considered in Refs. [2–4]. If $\delta\gamma$ is sufficiently small, the second term can be neglected, and the energy change will scale linearly with P. This is the case considered here.

The outline of the remainder of this paper is as follows. In Sec. II, we analyze the interaction between a relativistic electron and a two-frequency laser beam in vacuum. In Sec. III, we present three-dimensional numerical calculations of the effect of a two-frequency laser on a realistic electron beam. These calculations include radial and space charge effects not accounted for by the paraxial analysis. Finally, in Sec. IV, we numerically simulate the compression of a laser-modulated electron beam with space charge by a magnetic compression device.

II. PARAXIAL THEORY

We wish to determine the net change in the momentum of a highly relativisitic electron injected directly down the axis of a two-frequency laser beam. In the purely one-dimensional limit, the momentum of the electron will never converge to a stable value since the laser fields persist throughout all space. A paraxial model must be used in which the fields due to a Gaussian beam are expanded linearly about the axis of propagation [5]:

$$E_x = E_0 \frac{w_0}{w} \cos\Phi \cos\phi, \tag{4a}$$

$$E_z = 2E_0 \frac{w_0}{w} \frac{x}{kw^2} \cos\Phi \left(\sin\phi - \frac{z}{z_0} \cos\phi \right), \tag{4b}$$

$$B_y = E_0 \frac{w_0}{w} \cos\Phi \cos\phi, \tag{4c}$$

$$B_z = 2E_0 \frac{w_0}{w} \frac{y}{kw^2} \cos\Phi \left(\sin\phi - \frac{z}{z_0} \cos\phi \right). \tag{4d}$$

Here w_0 is the spot size at best focus, z_0 is the Rayleigh length, $w = w_0(1 + z^2/z_0^2)^{1/2}$ is the spot size at a given z, k is the average wave number of the two laser lines, ϕ is the phase relative to an optical cycle, and Φ is the phase relative to the beat pattern. The phase variables are expressed in terms of the coordinates of the electron,

$$\phi = \phi_0 + \kappa z, \tag{5}$$

$$\Phi = \Phi_0 + Kz, \tag{6}$$

where

$$\kappa = k\left(\frac{1}{\beta_z} - 1 \right) \approx \frac{k}{2\gamma^2}, \tag{7}$$

$$K = \frac{\Delta k}{2}\left(\frac{1}{\beta_z} - 1 \right) \approx \frac{\Delta k}{4\gamma^2}, \tag{8}$$

and Δk is the wave-number difference between the two laser lines. Here we assume that any perturbations to the axial momentum of the electron do not appreciably change its velocity. Also, the well known π phase shift through the laser's focal region is neglected [6]. These assumptions are removed in Sec. III, where it is found *a postiori* that they are valid.

To compute the axial forces on the electron its transverse motions must first be specified. In so far as the problem is nearly one dimensional, conservation of canonical momentum implies that

$$v_x = -\frac{a(z)c}{\gamma} \sin\phi, \tag{9}$$

where $a(z)$ is the slowly varying part of the normalized vector potential. That is,

$$a(z) = a_0 \frac{w_0}{w} \cos\Phi, \tag{10}$$

where

$$a_0 = \frac{eE_0}{kmc^2}. \tag{11}$$

The transverse position of the electron is then computed from

$$\beta_z c \frac{dx}{dz} = v_x \Rightarrow x = \frac{a(z)}{\beta_z \kappa \gamma} \cos\phi \approx \frac{2\gamma}{k} a(z) \cos\phi. \tag{12}$$

This imposes the requirement that $a_0 \ll kw_0/\gamma$, since otherwise the electron would be radially ejected from the laser beam.

The axial momentum of the electron evolves according to

$$\frac{dp_z}{dz} = -\frac{e}{c}\left(\frac{v_x}{c} B_y + E_z \right), \tag{13}$$

since $v_z \approx c$. Dividing both sides by mc results in the normalized equation

$$\frac{d\gamma}{dz} = -\frac{e}{mc^2}\left(\frac{v_x}{c} B_y + E_z \right), \tag{14}$$

where, strictly speaking, $\gamma = p_z/mc$. Note, however, that according to Eq. (9) the transverse momentum of the electron eventually vanishes. It follows that γ will eventually converge to the relativistic Lorentz factor associated with the electron, provided $\gamma \gg 1$.

In analyzing Eq. (14), it is useful to write out the $\mathbf{v}\times\mathbf{B}$ term separately from the electric field term. Substituting Eqs. (4c) and (9) into Eq. (14), we find that

$$\left(\frac{d\gamma}{dz} \right)_{\mathbf{v}\times\mathbf{B}} = \frac{k}{2\gamma} a(z)^2 \sin(2\phi). \tag{15}$$

Substituting Eq. (12) into Eq. (4b), and inserting the result into Eq. (14), we find that

$$\left(\frac{d\gamma}{dz} \right)_{E_z} = \frac{k}{2\gamma} a(z)^2 \left[\frac{z}{z_0}(1 + \cos 2\phi) - \sin 2\phi \right] \epsilon(z), \tag{16}$$

where

$$\epsilon(z) = \frac{2}{k\kappa w^2}. \tag{17}$$

The parameter ϵ compares the peak force exerted by the axial electric field with that exerted by the $\mathbf{v}\times\mathbf{B}$ force. This quantity is maximized at the origin, where

$$\epsilon(0) = \frac{1}{\kappa z_0} \approx \left(\frac{\lambda}{w_0} \frac{\gamma}{\pi} \right)^2. \tag{18}$$

More significantly, inspection of Eq. (16) shows that the force exerted by the electric field contains a slowly varying

term. This term arises due to the fact that the quiver excursion is in phase with one of the axial electric field terms, which itself contains the quiver excursion. The effect of the slowly varying term is to continuously push the electron away from best focus.

The final state of the electron is found by putting together Eqs. (15) and (16) and integrating over the whole line:

$$\delta\gamma=\frac{k}{2\gamma}\int_{-\infty}^{\infty}a(z)^2\left[\epsilon\frac{z}{z_0}(1+\cos 2\phi)+(1-\epsilon)\sin 2\phi\right]dz. \tag{19}$$

This integral can be approximated by discarding the rapidly varying terms. The error caused by this neglect is estimated as follows. Consider, for example, the $\mathbf{v}\times\mathbf{B}$ term over a finite interval of integration:

$$I=\frac{k}{2\gamma}\int_{z_1}^{z_2}a(z)^2\sin(2\kappa z)dz. \tag{20}$$

If the integration interval is small enough, $a(z)^2$ can be replaced by its second order Taylor expansion, in which case

$$I=\frac{k}{2\gamma}\frac{1}{4\kappa^2}(z_2-z_1)\frac{d^2}{dz^2}a(z)^2, \tag{21}$$

provided the limits of integration are selected from the discrete set of values $(n+1/2)\pi/\kappa$, where n is an integer. This particular integration interval can only be made small in the sense required above if the electron slips through many laser wavelengths while passing through the interaction region. That is, we require $\kappa z_0\gg 2\pi$ or, equivalently, $\gamma^2\ll kz_0/4\pi$. If this relation holds, expression (21) can in principle be summed over many small intervals to yield the value of the integral over the whole line. An estimate for this quantity is determined by applying Eq. (21) to an interval of π Rayleigh lengths centered at the origin. If the beat envelope is phased such that the second derivative of $a(z)^2$ is maximized in this interval, we obtain

$$(\delta\gamma)_{\text{fast}}=\frac{\pi}{2\gamma c}\left(\frac{e}{mc^2}\right)^2 P\left(\frac{\Delta k^2}{k^2}+\epsilon(0)^2\right), \tag{22}$$

where P is the average power in the beat pattern.

Next, we evaluate the slowly varying term

$$\delta\gamma=\frac{k}{2\gamma}\int_{-\infty}^{\infty}a(z)^2\epsilon(z)\frac{z}{z_0}dz. \tag{23}$$

Integration by parts yields

$$\delta\gamma=\frac{a_0^2}{2\gamma}\frac{z_0}{\kappa w_0^2}\left\{-\left[\frac{\cos^2\Phi}{w^2}\right]_{-\infty}^{\infty}-K\int_{-\infty}^{\infty}\sin 2\Phi\left(1+\frac{z^2}{z_0^2}\right)^{-1}dz\right\}. \tag{24}$$

The first term in the curly braces obviously vanishes. The second can be evaluating by using a linear expansion of the sine function about the origin. This is justified if the electron slips very little with respect to the beat pattern over a Rayleigh length, or, equivalently, if $\gamma^2\gg\Delta kz_0/8\pi$. In this case,

$$\delta\gamma=\frac{a_0^2}{2\gamma}\frac{z_0}{\kappa w_0^2}K\int_{-\infty}^{\infty}(\sin 2\Phi_0+Kz\cos 2\Phi_0)\left(1+\frac{z^2}{z_0^2}\right)^{-1}dz. \tag{25}$$

The cosine term vanishes since it is odd. The sine can be pulled outside the integral. The remaining integral is well known to equal πz_0. Rearranging various terms, we find that

$$\delta\gamma=-\frac{\pi}{2\gamma c}\left(\frac{e}{mc^2}\right)^2 P\frac{\Delta k}{k}\sin 2\Phi_0. \tag{26}$$

Expressing the laser power in terawatts, we have, for an electron,

$$\delta\gamma=-\frac{180}{\gamma}(P[\text{TW}])\frac{\Delta k}{k}\sin 2\Phi_0. \tag{27}$$

Comparison of Eqs. (26) and (22) shows that the contribution of the rapidly varying terms is indeed negligible provided that $\Delta k/k$ is small, and $\epsilon(0)^2\ll\Delta k/k$. In other words, there must be many optical cycles within a beat period, and the electron must slip through many optical cycles within the interaction region. This latter requirement is qualitatively the same as the one discussed in the context of Eq. (22), but now takes the form $\gamma^2\ll z_0\sqrt{k\Delta k}/2$, which is more strict than the previous relation. For the reader's convenience, Table I summarizes the inequalities involved in obtaining Eq. (26).

TABLE I. Bunching regime.

Requirement	Reason
$\gamma\gg 1$	Axial velocity constant
$\Delta k/k\ll 1$	Allow neglect of rapidly varying forces
$\gamma^2\ll z_0\sqrt{k\Delta k}/2$	Allow neglect of rapidly varying forces
$\gamma^2\gg\Delta kz_0/8\pi$	Linear expansion of beat envelope
$a_0\ll kw_0/\gamma$	Keep electron near the laser axis

Equation (26) indicates that the energy perturbation is dependent on the electron's phase with respect to the beat pattern at best focus. For a constant stream of electrons, this obviously translates into the foretold temporal modulation. Equation (26) also reveals that the energy perturbation does not depend on how tightly the laser is focused, despite the fact that only the axial fields were kept in the calculation. Evidently, as the one-dimensional limit is approached, the interaction region becomes longer in the same degree that the axial fields become smaller.

III. NUMERICAL CALCULATIONS

The above analytical model suffers from two basic limitations. First, it neglects radial effects. Second, it requires that a large number of quiver motions be executed within the interaction region. We overcome these limitations using a three-dimensional (3D) numerical calculation in which each particle of a realistic electron beam is independently pushed through a known laser field. The field due to each laser line is described by the following set of equations [5]:

TABLE II. Simulation parameters.

CO_2 Laser		Electron beam	
Power	2.5 TW	Current	30 A
Wavelength	10.3, 10.6 μm	Energy	16 MeV $\pm$ .025%
Rayl. len. (z_0)	1.2 cm	Emittance	0.01π mm mrad
Best focus (w_0)	200 μm	Best focus	50 μm

$$E_x = E_0 \frac{w_0}{w} \exp\left(-\frac{r^2}{w^2}\right) \cos\phi, \tag{28a}$$

$$E_z = 2E_0 \frac{w_0}{w} \frac{x}{kw^2} \exp\left(-\frac{r^2}{w^2}\right)\left(\sin\phi - \frac{z}{z_0}\cos\phi\right), \tag{28b}$$

$$B_y = E_0 \frac{w_0}{w} \exp\left(-\frac{r^2}{w^2}\right) \cos\phi, \tag{28c}$$

$$B_z = 2E_0 \frac{w_0}{w} \frac{y}{kw^2} \exp\left(-\frac{r^2}{w^2}\right)\left(\sin\phi - \frac{z}{z_0}\cos\phi\right), \tag{28d}$$

with the phase given by

$$\phi = kz - \omega t + \frac{r^2}{w^2}\frac{z}{z_0} - \tan^{-1}\left(\frac{z}{z_0}\right). \tag{29}$$

The total field is represented as the sum of the fields due to each laser line. The code also has a limited ability to simulate space charge forces. This is done by calculating the rms envelope of all the particles each time step, computing the dimensions of the equivalent uniform ellipsoid, and applying the space charge field as given by Lapostolle [7]. A numerical calculation much like the one described above (only without the space charge model) was applied in Ref. [4] to the regime appropriate to accelerator applications.

The experiment to be simulated is summarized in Table II. The electron beam is modeled after a 16-MeV photoinjector linac currently under construction at UCLA [8]. The optical beam is a 2.5-TW CO_2 laser running on the 10.6- and 10.3-μm lines such as the one under construction at Brookhaven [9]. Tentatively applying Eq. (26) to the parameters of Table II predicts an energy perturbation of approximately 1.2%. Further scrutiny, however, reveals that these parameters begin to test the limits of the analytical model. The number of optical cycles slipped through within the interaction region is on the order of unity, and the electron waist may be large enough to lead to measureable radial effects.

To isolate the effects of the slow slippage rate, we inject a single on-axis electron. It is phased such that when it reaches best focus it sits at the maximum gradient of the beat pattern. The electron's track through longitudinal phase space is shown in Fig. 1. The final energy perturbation is 1%, which is closer to the analytically predicted value than one might expect given the value of $\epsilon(0)$ for the parameters being modeled. Evidently, the rapidly oscillating forces contribute even less to the final energy perturbation than expected. This is

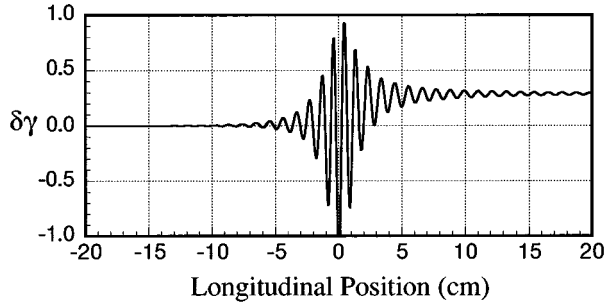

FIG. 1. The track left by an individual particle through longitudinal phase space. The particle is phased for maximum energy gain.

demonstrated in Fig. 2, which shows three tracks, each isolating the effects of one of three terms in the overall longitudinal force. As predicted, the part of the axial electric field in phase with the quiver excursion [Fig. 2(a)] exerts a unidirectional force resulting in a substantial energy gain. The part of the electric field out of phase with the quiver excursion [Fig. 2(b)] causes a much smaller energy loss. The $\mathbf{v}\times\mathbf{B}$ force has no noticeable net effect [Fig. 2(c)].

Next, we inject the electron beam described in Table II. The particles are copropagated 40 cm with the laser beam,

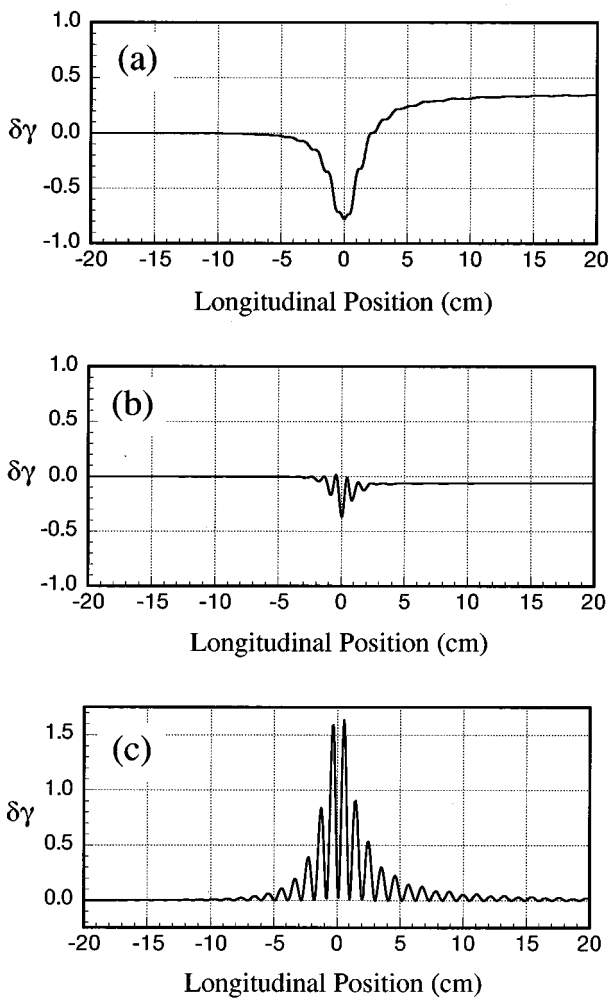

FIG. 2. Decomposition of longitudinal forces: (a) term of E_z in phase with E_x; (b) term of E_z out of phase with E_x; (c) longitudinal $\mathbf{v}\times\mathbf{B}$ force.

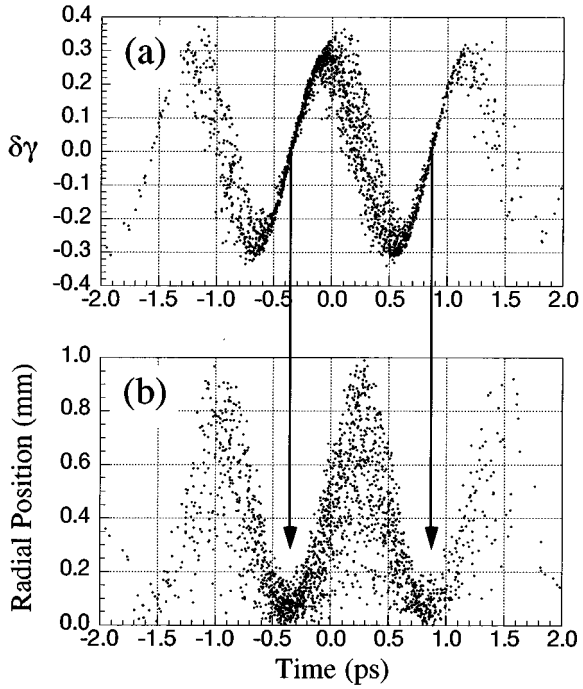

FIG. 3. Temporal structure of the beam 20 cm beyond focus: (a) longitudinal phase space structure; (b) correlation between radial blowout and time. The arrows emphasize that the temporally compressing particles can be identified with the minimally blown-out particles.

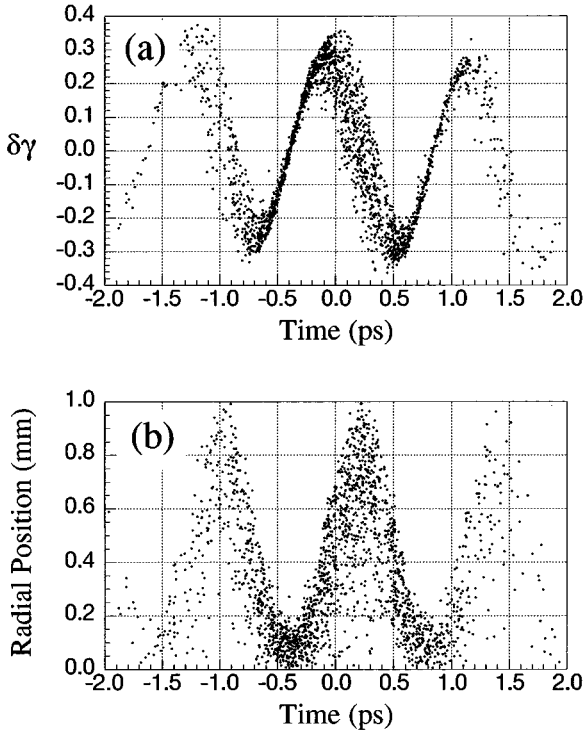

FIG. 4. Temporal structure of a 40-pC pulse at +20 cm: (a) longitudinal phase space structure; (b) correlation between radial blowout and time.

whose focus occurs at the midpoint of the interaction. Space charge is neglected. Figure 3 shows the temporal structure of the beam at the end of the 40 cm. Figure 3(a) shows that in addition to acquiring the expected momentum modulation, the beam is longitudinally heated in regions where the average momentum decreases with time. Figure 3(b) shows that, coincident with the longitudinal heating, radial ponderomotive blowout occurs. The correlation between radial blowout and time follows simply from the periodicity of the pondermotive force in a beat pattern. The correlation between blowout and longitudinal heating follows from the fact that the interaction between the particle and the laser is cut short if the particle exits the laser radially. A shortened interaction region makes it possible for the rapidly oscillating axial forces to permanently change the electron's momentum. Since the exact momentum change depends on the particle's phase within an optical cycle—an effectively random quantity—the beam heats up.

Finally, we inject 40 pC of electrons at 30 A. Figure 4 shows the temporal structure of the beam, again evaluated 20 cm from the focus. The space charge effects are not severe. The longitudinal phase structure aquires a small overall slope, while the radial structure is nearly identical to the one shown in Fig. 3. Unfortunately, this space charge calculation is not entirely correct since it averages over any density fluctuations within the beam. This is appropriate in the half space before the focus, but several centimeters beyond the focus the beam begins to acquire the longitudinal density modulation implied by Fig. 4(b). This inhomogeneity throws off the space charge calculation during the last few centimeters of the interaction. Nevertheless, because this error accumulates over only about 25% of the interaction length, Fig. 4 represents a reasonable estimate of the overall space charge effect.

IV. COMPRESSION

A beam for which momentum is an increasing function of time will automatically compress as it propagates. In particular, the laser-modulated beams described above will reach a longitudinal waist after propagating a distance given by

$$L=\frac{c}{P}\left(\frac{mc^2}{e}\right)^2\gamma^4\frac{k}{\Delta k^2}=\frac{0.009}{P[\mathrm{TW}]}\gamma^4\frac{k}{\Delta k^2}. \tag{30}$$

Using the parameters of Table II, for example, a longitudinal waist is reached after approximately 7 m. However, any reasonable amount of charge on the beam will prevent effective compression because of space charge forces acting over such a long drift space [10]. A magnetic compression system can overcome this problem by bringing the beam to a waist more suddenly. One such system is the chicane compressor [11] shown in Fig. 5. A chicane consists of four rectangular dipole magnets which cause low energy particles to trace out a longer path than high energy particles to get between the

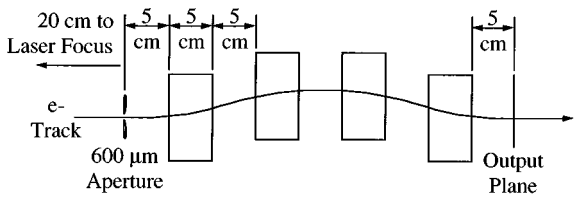

FIG. 5. Chicane compressor. The rectangles are the pole pieces of the magnets.

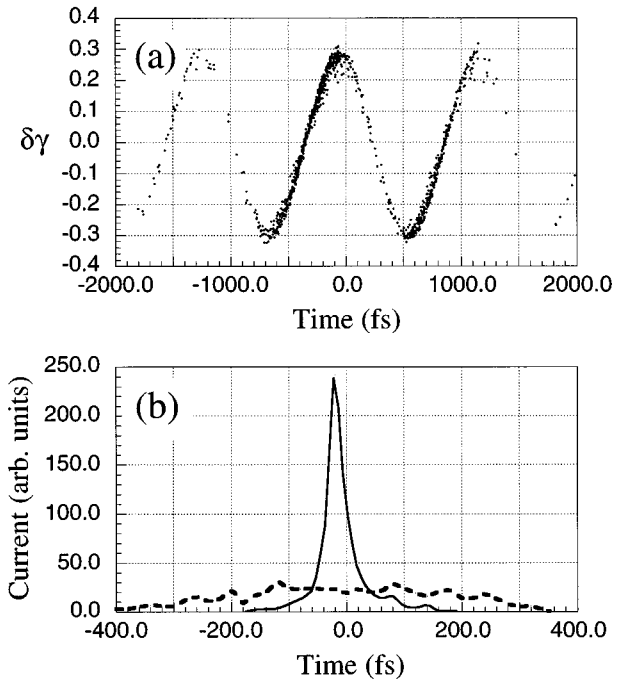

FIG. 6. Compression of zero charge beam: (a) longitudinal phase structure after 600-μm aperture; (b) one of the buckets before (dashed line) and after (solid line) compression.

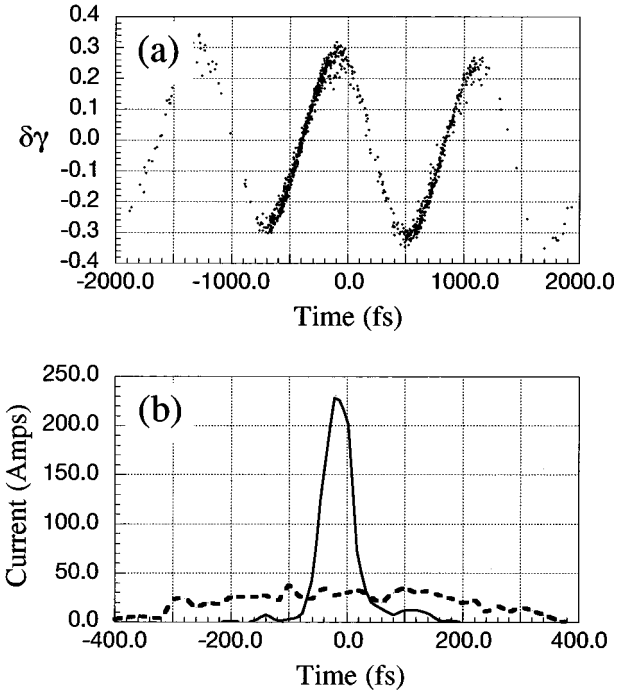

FIG. 7. Compression of the 40-pC beam: (a) longitudinal phase structure after 600-μm aperture; (b) one of the buckets before (dashed line) and after (solid line) compression. The particular bucket shown in (b) contains 10 pC.

same two points. This compresses regions of the beam where the momentum increases with time.

In the case of the laser-modulated beams described above, the particles for which momentum decreases with time can be eliminated using an aperture, since these are the same particles that get expanded radially. For our specific system a 600-μm aperture is placed 20 cm from the laser focus. The first chicane pole face is placed 5 cm from the aperture. We consider the effect of this system on the electron beams described by Figs. 3 and 4.

To model propagation through the chicane, we again use a 3D computer code. The fringing fields of the four dipoles are modeled according to the prescription of Enge [12]. The gap width of the dipoles is chosen to be 2 cm. Space charge is modeled as before, only now we run one ''bucket'' of electrons at a time. This is appropriate since as each bucket compresses, its own space charge field will affect it much more than the fields due to other buckets. Figure 6 shows the result of running the zero-charge beam from Fig. 3 through the system. The field in the dipoles was 1.6 kG. In Fig. 6(a), the longitudinal phase structure immediately after the 600-μm aperture is depicted. This merely emphasizes that nearly all the unwanted particles are eliminated by the aperture. In Fig. 6(b), the current distribution associated with the first bucket is shown before and after the chicane. The compressed pulse is about 40-fs full width at half maximum (FWHM). Figure 7 shows the result of running the 40 pC pulse from Fig. 4 through the system. The field in the dipoles was 1.75 kG. The compressed pulse in this case is about 60-fs FWHM, and contains 10 pC of charge.

The limits on effective compression are determined by the depth of the laser-induced momentum modulation, the longitudinal electron temperature, and the charge. In the zero-charge case, the maximum compression ratio is given simply by

$$\frac{I_{\text{compressed}}}{I_0} = \min\left\{\frac{\delta\gamma}{\sigma_\gamma}, 7\right\}, \tag{31}$$

where σ_γ represents the longitudinal temperature of the electrons. The factor of 7 is the largest compression ratio attainable given a sinusoidal velocity perturbation [13]. Nevertheless, in the case of Fig. 6, for example, the compression ratio is about 10. This suggests that, remarkably, the velocity perturbation induced by the laser contains some of the harmonics of a sawtooth wave. In the case of finite space charge, computer modeling shows that at around 100 A the effectiveness of the chicane starts to be seriously limited. For a more complete discussion of space charge effects on a compressing electron bunch, see Ref. [10].

V. CONCLUSIONS

A high power two-frequency laser can be used to modulate the momentum of a relativistic electron beam. The mechanism described in this work specializes to the case in which electrons slip through many optical cycles but only a fraction of a beat cycle while passing through the interaction region. The axial electric field of the laser plays a crucial role even for a large laser spot size or, equivalently, high f-number focusing. Computer modeling shows that a 2.5-TW CO_2 laser combined with a chicane compressor can transform a 30-A beam of 16-MeV electrons into a train of 60 fs microbunches each containing 10 pC. This method of microbunch formation looks particularly attractive for inject-

ing and phase locking the electrons in the plasma beatwave accelerator which is driven by the same two-frequency laser beam. Experimental realization of this scheme would represent an interesting first demonstration of useful laser acceleration in vacuum.

ACKNOWLEDGMENTS

We would like to thank J. Rosenzweig for the design of the chicane. This work was supported by DOE Grant No. DE-FG03-92ER40727.

[1] T. Tajima and J. M. Dawson, Phys. Rev. Lett. **43**, 267 (1979).
[2] P. Sprangle *et al.*, Opt. Commun. **124**, 69 (1996).
[3] E. Esaray *et al.*, Phys. Rev. E **52**, 5443 (1995).
[4] B. Hafizi *et al.*, Phys. Rev. E **55**, 5924 (1997).
[5] Expressions for E_x and B_y are found, for example, in A. Siegman, *Lasers* (University Science Books, California, 1986). The axial fields are then found from $\nabla \cdot \mathbf{E} = 0$ and $\nabla \cdot \mathbf{B} = 0$.
[6] We refer to the Guoy phase shift which results in a phase velocity greater than c in and near the focal region of a laser beam. See, for example, A. Siegman, *Lasers* (Ref. [5]).
[7] P. M. Lapostolle, CERN Report No. AR/Int. SG/65-15, Geneva, Switzerland, 1965 (unpublished).
[8] S. Hartman *et al.*, Nucl. Instrum. Methods Phys. Res. A **340**, 219 (1994).
[9] I. V. Pogorelsky *et al.* (unpublished).
[10] T. Katsouleas *et al.*, IEEE Trans. Plasma Sci. **24**, 443 (1996).
[11] J. B. Rosenzweig *et al.*, IEEE Trans. Plasma Sci. **24**, 409 (1996).
[12] H. Enge, in *Focusing of Charged Particles*, edited by A. Septier (Academic, New York, 1967), Chap. 4.2.
[13] T. Katsouleas (private communication).